

Correlation between Functionality Preference of Ru Carbenes and *exo/endo* Product Selectivity for Clarifying the Mechanism of Ring-Closing Enyne Metathesis

Ok Suk Lee,[†] Kyung Hwan Kim,^{‡,§} Jinwoo Kim,[‡] Kuktae Kwon,[‡] Taedong Ok,^{||} Hyotcherl Ihee,^{*,‡,§} Hee-Yoon Lee,^{*,‡} and Jeong-Hun Sohn^{*,†}

[†]Department of Chemistry, College of Natural Sciences, Chungnam National University, Daejeon 305-764, Korea

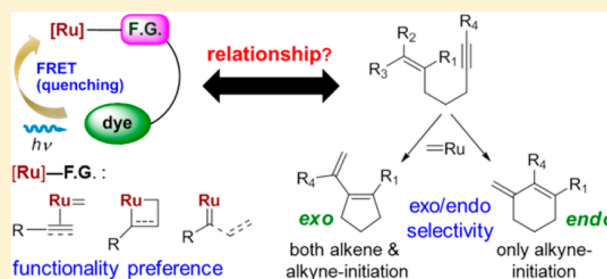
[‡]Department of Chemistry, KAIST, Daejeon 305-701, Korea

[§]Center for Nanomaterials and Chemical Reactions, Institute for Basic Science, Daejeon 305-701, Korea

^{||}College of Medicine, Yonsei University, Seoul 120-752, Korea

S Supporting Information

ABSTRACT: Functionality preferences of metathesis Ru carbenes to various alkenes and alkynes with electronic and steric diversity were determined by using time-dependent fluorescence quenching. The functionality preferences depend not only on the properties of multiple bonds but also on the ligands on Ru. There was a good correlation between functionality preference and the metathesis reaction outcome. The correlation between functionality preference and *exo/endo* product ratio offers a solution to resolve the mechanistic issue related with alkene- vs alkyne-initiated pathway in ring-closing enyne metathesis. The correlation indicates the preference is likely to dictate the reaction pathway and eventually the outcome of the reaction. The Ru catalyst favoring alkyne over alkene provides more *endo* product, indicating that the reaction mainly initiates at the alkyne. By changing the substitution pattern, the preference can be reversed to give an exclusive *exo* product.



INTRODUCTION

Fluorescence resonance energy transfer (FRET) is a distance-dependent interaction and is detected by the fluorescence appearance from the fluorescence acceptor or by quenching of the fluorescence from the fluorescence donor.¹ Many transition metal complexes exhibit their own visible colors, meaning that their absorbance or emission bands are at the visible light range. We conceived that the colored metal complex could act as either fluorescence donor, acceptor, or quencher for dyes due to FRET phenomenon, when complexed with a dye-conjugated functionality (Figure 1). By measurement of fluorescence quenching as a function of time, both kinetic and thermodynamic preference of the metal complex toward the

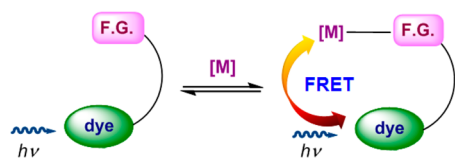


Figure 1. Schematic illustration of the FRET-based method to determine the functionality preference of metal complexes having visible colors. The metal complexes could act as either fluorescence donor, acceptor, or quencher for dyes due to FRET phenomenon, when complexed with a dye-conjugated functionality.

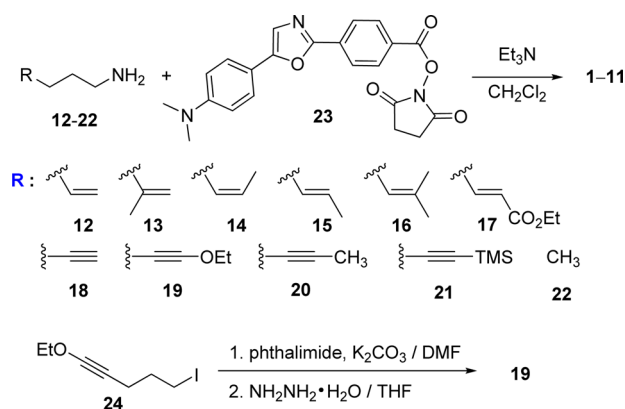
functional groups, which reflects the early event in the reaction, can be determined. In metal-catalyzed coupling reactions with multiple functionalities, the catalyst-functionality complex formation might be critical to determine overall reaction pathway and final product. Using this FRET-based method, we have endeavored to solve the mechanistic ambiguity in ring-closing enyne metathesis (enyne RCM) that provides undisputed efficiencies in producing synthetically versatile cyclic 1,3-dienes.² Mo or Ru carbene complexes for metathesis reaction have absorbance bands at visible range and do not emit fluorescence. We previously demonstrated that these catalysts act as fluorescence quenchers for the dyes conjugated with terminal alkene, alkyne, and allene through the formation of catalyst-substrate complexes.³

The mechanistic ambiguity of the enyne RCM reactions, especially catalyzed by Ru complexes, has attracted much attention and debate for the following reasons.^{2g,4} First, there exist two equally plausible mechanisms for the formation of the same *exo* product via the reaction initiation either at the alkene (Route A of Scheme 1)⁵ or at the alkyne (Route B).⁶ Second, extensive research on enyne RCM has established that the *exo* product is formed exclusively.² There has been no report on the

Received: July 2, 2013

Published: August 14, 2013

Scheme 2. Syntheses of Dapoxyl-Cojugated Alkenes and Alkynes



for only a single kind of the initial catalyst. We measured the time-dependent fluorescence quenching of each of various pairs of ten substrates (10–25 μM) and two catalysts (1.5–3.0 equiv) in CH_2Cl_2 at 20 $^\circ\text{C}$. An example of the fluorescence traces is shown in Figure 3. These are the calibrated integrated values of the corresponding fluorescence spectra for all used combinations of the ten substrates (20 μM) and the two catalysts (1.5 equiv) over 20 min.

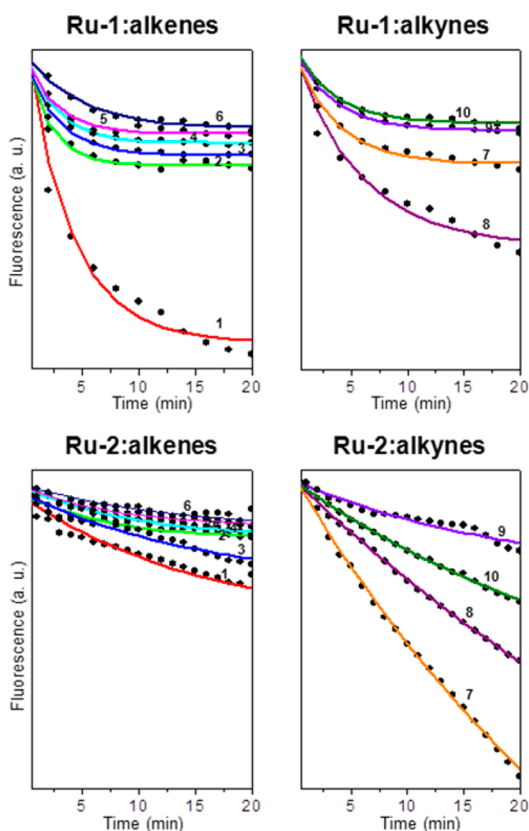


Figure 3. Time-dependent fluorescence quenching of the substrates (alkenes 1–6 and alkynes 7–10) by the catalysts, **Ru-1** and **Ru-2**. Experimental data points are shown as black circles (20:30 μM of substrates vs catalysts), which correspond to the integrated values of the fluorescence spectra (see Supporting Information for details). The theoretical curves from the fitting analysis³ are represented as red (1), green (2), blue (3), cyan (4), magenta (5), navy (6), orange (7), purple (8), violet (9), and olive (10).

For each catalyst, the fluorescence quenching traces were quantitatively analyzed with a set of parameters to determine both kinetic and thermodynamic parameters, k , k_{-1} , and ΔG , of formation of the Ru-substrate complex for a given substrate/catalyst pair; the results are summarized in Table 1.

Table 1. Kinetic and Thermodynamic Parameters for Alkenes and Alkynes with Ru Catalysts^a

catalyst	substrate	k ($\text{M}^{-1} \text{s}^{-1}$)	k_{-1} (s^{-1})	ΔG (kJ/mol)	rel. stability ^b
Ru-1	1	$3.15 (\pm 0.19) \times 10^3$	$2.21 (\pm 0.33) \times 10^{-2}$	-28.9 ± 0.39	1
	2	$2.07 (\pm 0.30) \times 10^3$	$3.70 (\pm 0.61) \times 10^{-1}$	-21.4 ± 0.54	0.740
	3	$1.36 (\pm 0.22) \times 10^3$	$2.84 (\pm 0.49) \times 10^{-1}$	-21.0 ± 0.59	0.726
	4	$1.27 (\pm 0.20) \times 10^3$	$2.93 (\pm 0.56) \times 10^{-1}$	-20.8 ± 0.61	0.720
	5	$1.15 (\pm 0.19) \times 10^3$	$3.12 (\pm 0.60) \times 10^{-1}$	-20.4 ± 0.63	0.706
	6	$6.34 (\pm 0.97) \times 10^2$	$1.73 (\pm 0.37) \times 10^{-1}$	-20.3 ± 0.65	0.702
	7	$1.44 (\pm 0.15) \times 10^3$	$1.33 (\pm 0.24) \times 10^{-1}$	-22.6 ± 0.40	1
	8	$1.65 (\pm 0.19) \times 10^3$	$1.02 (\pm 0.12) \times 10^{-1}$	-24.0 ± 0.41	1.062
	9	$1.04 (\pm 0.14) \times 10^3$	$2.28 (\pm 0.37) \times 10^{-1}$	-20.9 ± 0.52	0.925
	10	$9.80 (\pm 1.38) \times 10^2$	$2.30 (\pm 0.40) \times 10^{-1}$	-20.7 ± 0.55	0.916
Ru-2	1	$2.57 (\pm 0.49) \times 10^2$	$4.78 (\pm 1.25) \times 10^{-2}$	-21.3 ± 0.65	1
	2	$1.72 (\pm 0.92) \times 10^2$	$5.24 (\pm 1.79) \times 10^{-2}$	-19.7 ± 0.85	0.925
	3	$1.84 (\pm 0.28) \times 10^2$	$5.27 (\pm 1.51) \times 10^{-2}$	-20.2 ± 0.71	0.950
	4	$1.67 (\pm 0.46) \times 10^2$	$9.11 (\pm 1.74) \times 10^{-2}$	-18.6 ± 0.47	0.875
	5	$1.48 (\pm 0.50) \times 10^2$	$1.08 (\pm 0.43) \times 10^{-1}$	-17.9 ± 0.99	0.841
	6	$1.10 (\pm 0.41) \times 10^2$	$7.16 (\pm 1.85) \times 10^{-2}$	-18.2 ± 0.64	0.855
	7	$6.31 (\pm 2.64) \times 10^2$	$4.76 (\pm 0.82) \times 10^{-4}$	-34.9 ± 0.43	1
	8	$3.56 (\pm 1.48) \times 10^2$	$1.37 (\pm 0.47) \times 10^{-3}$	-30.9 ± 0.85	0.885
	9	$1.58 (\pm 0.30) \times 10^2$	$2.81 (\pm 1.31) \times 10^{-2}$	-21.0 ± 0.81	0.602
	10	$2.64 (\pm 0.37) \times 10^2$	$1.91 (\pm 0.28) \times 10^{-2}$	-23.6 ± 0.36	0.677

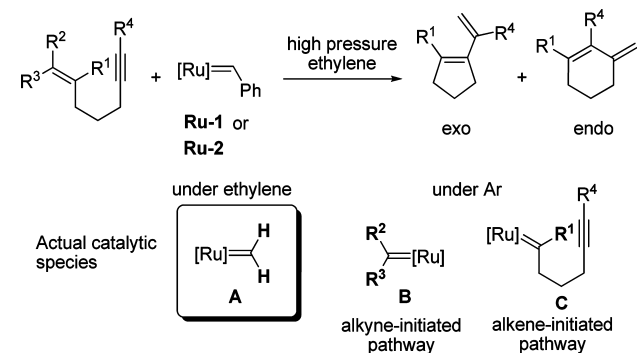
^a k and k_{-1} are directly determined as fitting parameters, and ΔG is calculated as $-RT \ln(k/k_{-1})$. k and ΔG represent the kinetic and thermodynamic preferences, respectively. ^bRelative thermodynamic stability of the catalyst–substrate complexes. The ΔG values of catalyst–alkene (1) complexes and catalyst–alkyne (7) complexes are defined as 1. The thermodynamic functionality preference of **Ru-1** is $1 > 8 > 7 > 2 > 3 > 9 > 4 > 10 > 5 > 6$, while that of **Ru-2** is $7 > 8 > 10 > 1 > 9 > 3 > 2 > 4 > 6 > 5$.

Since formation of the intermediates is reversible in the enyne RCM, the thermodynamic functionality preference (ΔG) is more important than the kinetic preference. A more negative ΔG value indicates a stronger thermodynamic preference. For alkene substrates, the functionality preferences of both **Ru-1** and **Ru-2** catalysts follow the substitution number of the alkenes, as anticipated, i.e., terminal > monomethylated > dimethylated alkene. On the other hand, the electron-deficient alkene 6 is least preferred by **Ru-1** but is positioned prior to the dimethylated alkene 5 in the case of **Ru-2**. Among the three

monomethylated alkenes, the two catalysts exhibit different preference orders, i.e., 2-methylated (2) > *cis*-methylated (3) > *trans*-methylated alkene (4) for **Ru-1** and *cis*-methylated (3) > 2-methylated (2) > *trans*-methylated alkene (4) for **Ru-2**. The preference of the catalysts becomes more complex for alkyne than for alkene substrates. Interestingly, among alkyne substrates, **Ru-1** primarily prefers ethoxylated alkyne **8**, whereas **Ru-2** favors terminal alkyne **7**, and their preference orders are completely different. For all alkenes and alkynes investigated in this study, the overall thermodynamic functionality preference of **Ru-1** is alkene 1 > alkyne 8 > alkyne 7 > alkene 2 > alkene 3 > alkyne 9 > alkene 4 > alkyne 10 > alkene 5 > alkene 6, while that of **Ru-2** is alkyne 7 > alkyne 8 > alkyne 10 > alkene 1 > alkyne 9 > alkene 3 > alkene 2 > alkene 4 > alkene 6 > alkene 5. It is obvious that substituents on either alkene or alkyne have strong effects on the functionality preference of both catalysts, which is partially consistent with the previously calculated reactivity order for substituted alkenes and alkynes, although the order is not an exact match.¹⁶

After identifying the functionality preference, our efforts were then directed to the design of enyne RCM experiments whose product outcomes can be linked to the functionality preference. For this purpose, we considered that fixing the actual catalytic species as a single species during the reactions is critical to correlate the *exo/endo* selectivity with the functionality preference. Thus, we devised the reaction condition involving high ethylene pressure to ensure that a single catalytic species, the Ru-methylidene (**A** in Scheme 3), is operating during the

Scheme 3. Enyne RCM Reactions under High Ethylene Pressure

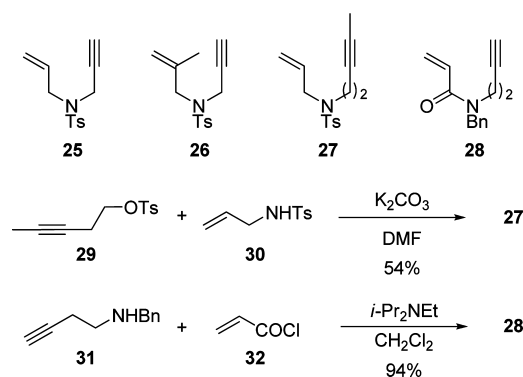


reaction cycles¹¹ and to divert the reaction pathways depending on the ene/yne preferences of the catalysts where we expect substrate-dependent *exo/endo* selectivity.¹⁷ Under Ar, the actual catalytic species is Ru complex, which is identified by enyne substrates and by the reaction pathway initiated at alkene (**B**) or alkyne (**C**) as shown in Scheme 3. Though the functionality preference of Ru methylidene complexes is more desirable than that of the precatalysts, **Ru-1** and **Ru-2**, in establishing the correlation, the experimental limitation only allowed the preference of the latter. However, it is likely that there is no significant deviation between the precatalysts and their methylidenes in the correlation, because we observed that the **Ru-1** analogue replacing benzylidene of **Ru-1** with isopentenylidene shows no change of the order of functionality preference to **Ru-1**.¹⁸

To investigate the *exo/endo* product ratios, we chose four representative enyne substrates containing different pairs of alkenes and alkynes, whose preferences toward both catalysts

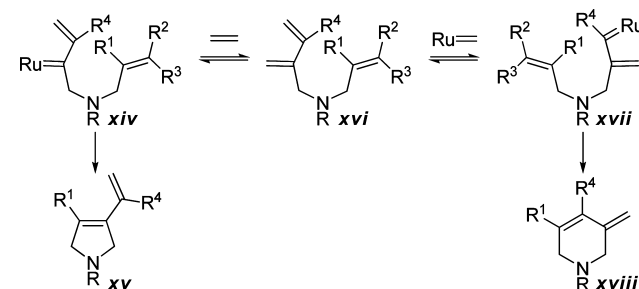
were determined by the FRET-based method. If the enynes react with the catalyst preferring the alkyne over the alkene and produce more of the *endo* product and/or the triene relative to the *exo* product, then it would be highly likely that the functionality preference guides the final outcome of the product. This conclusion would be further strengthened if the *exo/endo* selectivity variation correlates well with the change in the preference caused by the substituent effect. Enyne substrates **25**^{8b} and **26**¹⁹ having terminal alkene/terminal alkyne and methylated alkene/terminal alkyne, respectively, were prepared by following the literature procedures. Previously unknown substrates **27** and **28** containing terminal alkene/methylated alkyne and electron-deficient alkene/terminal alkyne, respectively, were synthesized as shown in Scheme 4.

Scheme 4. Enyne Substrates for Evaluation of *exo/endo* Product Ratio



We carried out RCM reactions of the enyne substrates using 5 mol % Ru catalyst in CH₂Cl₂ under ethylene pressure (100 psi) at 40 °C for 20 h. In addition to the production of the identical Ru methylidene in all reactions, the high ethylene pressure makes it possible to intercept intermediate **xiv**, a precursor to the *exo* product **xv**, as the triene **xvii** (Scheme 5).

Scheme 5. Possible Product Shift of *exo* to *endo* in the Alkyne-Initiated Pathways



The triene eventually transforms into the *endo* product **xviii**, resulting in the product shift of *exo* to *endo* in Routes B and C in Scheme 1, both of which are initiated at the alkyne site. The results of the enyne RCM reactions are summarized in Table 2.

Enyne **25** containing terminal alkene and terminal alkyne groups has been known to show a strong preference for the *exo* product in Ru-based reactions, regardless of the mechanistic pathway (Route A and B in Scheme 1).²⁰ Catalyst **Ru-1**, which prefers the terminal alkene **1** over the terminal alkyne **7**, produced only the *exo* product **33**.^{8b} However, with the alkyne-

Table 2. Variation of *exo/endo* Ratio in Enyne RCM Using Ru-1 and Ru-2^a

entry	substrate	conversion (%)	products			ratio (exo/endo/triene) ^c	
			exo	endo	triene	Ru-1	Ru-2
1		100				100/0/0	94/6/0
2		100				27/73/300	20/80/1
3		100				100/0/0	100/0/63
4		100 ^b				-	17/83/80

^aReactions were carried out under 100 psi of ethylene with 5 mol % of Ru catalyst in CH₂Cl₂ at 40 °C for 20 h. ^bSubstrate **14** was completely consumed by **Ru-2**, whereas most remained in the case of **Ru-1**. ^cRatios were determined by analysis of integration of the olefinic protons from the 400 MHz ¹H NMR spectra of crude mixtures.

favoring **Ru-2**, some *endo* product **34**^{8b} was obtained with an *exo/endo* ratio of 94/6 (Table 2, entry 1). The formation of the *endo* product in the reaction with **Ru-2** has a significant implication because it indicates that at least 6% of the product mixture was produced through reaction initiation at the alkyne (Route C and/or combination of Routes B and C).

The ratios of the products for both catalysts dramatically changed for enyne **26** having a 1,1-disubstituted alkene and a terminal alkyne. The reactions with both **Ru-1** and **Ru-2** yielded *endo* product **37**^{8b} as the major product over *exo* product **36**²¹ along with triene **38** (entry 2). The product ratios agree with the higher preference of both catalysts to the terminal alkyne 7 over the disubstituted alkene 2. The higher triene ratio with **Ru-1** also reflects the higher reactivity of **Ru-2** over **Ru-1** for the substituted alkene.

On the other hand, for enyne **27** having terminal alkene and methylated alkyne, for which both catalysts prefer the former functionality (1) to the latter (9), both catalysts yielded only *exo* product **39**²² with no *endo* product, and only **Ru-2** produced an appreciable amount of triene **41**²³ (entry 3). This difference between **Ru-1** and **Ru-2** in producing the triene product can be explained by the relative 1/9 functionality preference difference between **Ru-1** and **Ru-2**. The data in Table 1 show a preference difference of 4.2 kJ/mol for **1** and **9** for **Ru-1**, whereas **Ru-2** shows a much smaller value of 0.3 kJ/mol. Therefore, it is highly plausible that **Ru-1** allows only alkene-initiated pathway to form **39**, whereas the more reactive **Ru-2** allows both alkene- and alkyne-initiated pathways.

For the RCM of enyne **28** having terminal alkyne and electron-deficient acrylic alkene, an *exo/endo* product ratio of 17:83 together with the alkyne-transformed triene **44** was obtained with **Ru-2**, whereas starting material **28** was almost unreactive toward **Ru-1** (entry 4). In addition, when the reaction was evaluated under Ar, only *exo* product **42** was observed in a small amount. Instead, the triene **44** was obtained as the major product for **Ru-2**; most of the starting material

remained unreactive toward **Ru-1**. These results are in line with the product shift of *exo* to *endo* in Routes B and C in Scheme 1 under ethylene atmosphere.

Overall, the results in Tables 1 and 2 show good correlations between the functionality preference of the Ru catalyst and the *exo/endo* product ratio in the enyne RCM reactions. The correlation exhibits that the former is likely to govern the latter in Ru-catalyzed enyne RCM reactions. This means that the reactions proceed through either alkene- or alkyne-initiated pathways, which is dictated by the functionality preference of the catalyst (Figure 4). In other words, because the

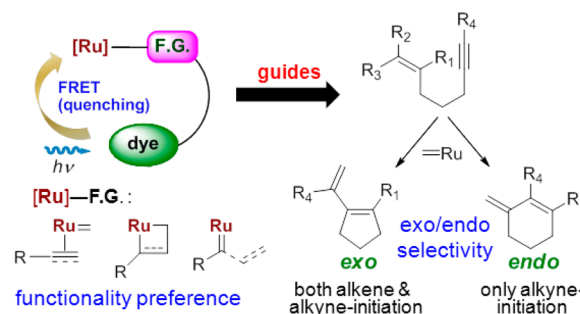


Figure 4. The correlation between functionality preference of Ru and *exo/endo* product ratio in Ru-based enyne RCM reaction. The correlation exhibited that the former is likely to govern the latter.

functionality preference reflects the feasibility of the generation of Ru-alkene/alkyne complexes *ii-iv* or *vii-xi*, the energetics for these intermediates determines the reaction pathway and the final product distribution.

CONCLUSION

We have determined the functionality preference of metathesis Ru catalysts toward diverse alkenes and alkynes by using time-dependent fluorescence quenching. The relative alkene/alkyne

functionality preference was applied to unravelling the mechanism of enyne RCM by correlating with *exo/endo* product selectivity in the Ru-based reactions. The correlation clearly shows that the former is likely to govern the latter and indicates that the reactions proceed through either alkene- or alkyne-initiated pathways, dictated by the functionality preference of the catalyst. For the RCM reaction of the enyne containing terminal alkene and terminal alkyne groups under identical steric and electronic environments, our results support the reaction pathway in which the reaction with **Ru-1** and **Ru-2** initiates preferably at the alkene and the alkyne, respectively. The results offer a rational design guide for tandem reaction methodologies using sequential metathesis processes dictated by the functionality preference of a catalyst, as well as a unified mechanistic explanation of the Ru-based enyne RCM reactions.

EXPERIMENTAL SECTION

General Methods. Common solvents were purified before use. Tetrahydrofuran (THF) and dichloromethane (CH_2Cl_2) were purified by distillation from sodium-benzophenone and calcium hydride, respectively. *N,N*-Dimethylformamide, acetonitrile and triethylamine were used as received. All reagents were reagent grade and purified where necessary. "Water" refers to distilled water. Reactions were monitored by thin layer chromatography (TLC) using silica gel plates. Flash column chromatography was performed over ultrapure silica gel (230–400 mesh). ^1H NMR and ^{13}C NMR spectra were recorded on a 400 or 600 MHz spectrometer using residual solvent peaks as an internal standard (CHCl_3 : δ 7.24 ppm for proton and δ 77.0 ppm for carbon; acetone: δ 2.05 ppm for proton and δ 29.9 ppm for carbon; benzene: δ 7.15 ppm for proton and δ 128.0 ppm for carbon; toluene: δ 2.09 ppm for proton and δ 20.4 ppm for carbon). Multiplicities for ^1H NMR are designated as follows: s = singlet, d = doublet, dd = doublet of doublets, ddd = doublet of dd, dt = doublet of triplets, ddt = doublet of dt, t = triplet, q = quartet, quint = quintet, m = multiplet, bs = broad singlet. Infrared spectra (IR) were recorded on FT-IR spectrometer and are reported in reciprocal centimeters (cm^{-1}). UV–visible spectra were recorded on UV–visible spectrophotometer. High resolution mass spectra (HRMS) were obtained on TOF-Q.

General Procedure for the Syntheses of Compounds 2–5, 9, and 10. To a mixture of amine **12**,²⁴ **13**,²⁵ **14**,²⁵ **15**,²⁶ **20**,²⁷ or **21**²⁸ (9.0 μmol) and activated dye **23** (6.2 μmol) in CH_2Cl_2 (0.2 mL) was added Et_3N (27 μmol), and the resulting mixture was stirred for 20 min at 0 °C. The mixture was diluted with EtOAc (3 mL), washed with saturated NH_4Cl (0.5 mL) and brine (0.5 mL), dried over MgSO_4 , filtered, and concentrated under reduced pressure. The crude product was purified by flash column chromatography or preparative TLC to give the desired dapoxy-conjugated product.

Compound 2. (2.1 mg, 87%): TLC (EtOAc:*n*-hexane, 50:50 v/v) R_f = 0.40; ^1H NMR (400 MHz, CDCl_3) δ 8.12 (d, J = 8.4 Hz, 2H), 7.84 (d, J = 8.5 Hz, 2H), 7.58 (d, J = 8.9 Hz, 2H), 7.26 (s, 1H), 6.74 (d, J = 9.0 Hz, 2H), 6.21 (m, 1H), 4.75 (m, 2H), 3.47 (q, J = 7.0 Hz, 2H), 3.01 (s, 6H), 2.13 (m, 2H), 1.77 (quint, J = 7.2 Hz, 2H), 1.74 (s, 3H); ^{13}C NMR (100 MHz, CDCl_3) δ 166.7, 159.6, 153.4, 151.0, 145.7, 136.1, 130.9, 130.0, 127.9, 126.7, 126.3, 121.7, 113.1, 111.3, 40.5, 40.0, 35.3, 29.7, 22.3; UV–vis λ_{max} 366 nm; Fluorescence λ_{max} (CH_2Cl_2) 508 nm; HRMS (ESI) (m/z) calcd for $\text{C}_{24}\text{H}_{28}\text{N}_3\text{O}_2$ [$\text{M} + \text{H}$]⁺ 390.2182, found 390.2183; IR (film) cm^{-1} 3853, 3748, 3673, 3650, 2923, 2851, 2359, 2340, 1734, 1699, 1651, 1613, 1558, 1540, 1509, 1364, 1197, 1106, 860, 815.

Compound 3. (2.3 mg, 95%): TLC (EtOAc:*n*-hexane, 50:50 v/v) R_f = 0.40; ^1H NMR (400 MHz, CDCl_3) δ 8.11 (d, J = 8.4 Hz, 2H), 7.83 (d, J = 8.4 Hz, 2H), 7.58 (d, J = 8.9 Hz, 2H), 7.25 (s, 1H), 6.74 (d, J = 8.9 Hz, 2H), 6.18 (m, 1H), 5.51 (m, 1H), 5.41 (m, 1H), 3.47 (q, J = 6.8 Hz, 2H), 3.01 (s, 6H), 2.16 (m, 2H), 1.71 (quint, J = 7.2 Hz, 2H), 1.62 (d, J = 6.2 Hz, 3H); ^{13}C NMR (100 MHz, CDCl_3) δ 166.7, 158.9, 152.8, 150.6, 135.4, 130.3, 129.4, 127.3, 126.0, 125.6, 125.0, 121.0, 115.8, 112.2, 40.3, 39.9, 29.3, 24.4, 12.8; UV–vis λ_{max} 366

nm; Fluorescence λ_{max} (CH_2Cl_2) 508 nm; HRMS (ESI) (m/z) calcd for $\text{C}_{24}\text{H}_{28}\text{N}_3\text{O}_2$ [$\text{M} + \text{H}$]⁺ 390.2182, found 390.2180; IR (film) cm^{-1} 3853, 3748, 3673, 3650, 2922, 2360, 2340, 1734, 1717, 1699, 1652, 1614, 1558, 1540, 1508, 1457, 668.

Compound 4. (2.2 mg, 92%): TLC (EtOAc:*n*-hexane, 50:50 v/v) R_f = 0.43; ^1H NMR (400 MHz, CDCl_3) δ 8.15 (d, J = 8.4 Hz, 2H), 8.02 (d, J = 8.4 Hz, 2H), 7.68 (d, J = 9.0 Hz, 2H), 7.46 (s, 1H), 6.85 (d, J = 9.0 Hz, 2H), 5.18 (dd, J = 6.0, 5.4 Hz, 1H), 3.42 (q, J = 6.6 Hz, 2H), 3.03 (s, 6H), 2.07 (m, 2H), 1.67 (s, 3H), 1.59 (s, 3H); ^{13}C NMR (100 MHz, CDCl_3) δ 166.7, 158.9, 152.8, 150.6, 135.5, 130.4, 130.3, 127.3, 126.0, 125.8, 125.7, 121.0, 115.8, 112.2, 40.3, 39.9, 30.2, 29.7, 29.3, 17.9; UV–vis λ_{max} 366 nm; Fluorescence λ_{max} (CH_2Cl_2) 508 nm; HRMS (ESI) (m/z) calcd for $\text{C}_{24}\text{H}_{28}\text{N}_3\text{O}_2$ [$\text{M} + \text{H}$]⁺ 390.2182, found 390.2183; IR (film) cm^{-1} 3853, 3748, 3673, 3650, 2922, 2360, 2340, 1734, 1717, 1699, 1652, 1614, 1558, 1540, 1508, 1457, 668.

Compound 5. (2.0 mg, 80%): TLC (EtOAc:*n*-hexane, 50:50 v/v) R_f = 0.50; ^1H NMR (600 MHz, acetone- d_6) δ 8.15 (d, J = 8.4 Hz, 2H), 8.03 (d, J = 8.4 Hz, 2H), 7.87 (bs, 1H), 7.69 (d, J = 8.9 Hz, 2H), 7.46 (s, 1H), 6.85 (d, J = 9.0 Hz, 2H), 5.18 (m, 1H), 3.42 (m, 2H), 3.03 (s, 6H), 2.08 (m, 2H), 1.67 (m, 5H), 1.59 (s, 3H); ^{13}C NMR (150 MHz, CDCl_3) δ 167.0, 158.9, 152.8, 135.2, 134.1, 130.3, 127.3, 126.0, 125.6, 121.0, 120.1, 119.5, 112.2, 44.3, 40.3, 30.9, 26.25, 26.20, 17.9; UV–vis λ_{max} 366 nm; Fluorescence λ_{max} (CH_2Cl_2) 508 nm; HRMS (ESI) (m/z) calcd for $\text{C}_{25}\text{H}_{29}\text{NaN}_3\text{O}_2$ [$\text{M} + \text{Na}$]⁺ 426.2152, found 426.2153; IR (film) cm^{-1} 3853, 3748, 3673, 3650, 2963, 2925, 2853, 2360, 2340, 1734, 1699, 1652, 1613, 1558, 1540, 1509, 1436, 1363, 1261, 1198, 1110, 951, 859, 816, 668.

Compound 9. (2.2 mg, 92%): TLC (EtOAc:*n*-hexane, 50:50 v/v) R_f = 0.35; ^1H NMR (400 MHz, CDCl_3) δ 8.11 (d, J = 8.5 Hz, 2H), 7.85 (d, J = 8.5 Hz, 2H), 7.58 (d, J = 8.9 Hz, 2H), 7.26 (s, 1H), 6.74 (d, J = 9.0 Hz, 2H), 6.57 (m, 1H), 3.59 (q, J = 6.4 Hz, 2H), 3.01 (s, 6H), 2.28 (m, 2H), 1.81 (m, 2H), 1.78 (t, J = 2.6 Hz, 3H); ^{13}C NMR (100 MHz, CDCl_3) δ 166.7, 158.9, 152.9, 150.6, 135.4, 130.3, 127.4, 126.0, 125.6, 121.0, 115.8, 112.2, 78.5, 76.9, 40.3, 39.9, 28.2, 16.8, 3.5; UV–vis λ_{max} 366 nm; Fluorescence λ_{max} (CH_2Cl_2) 508 nm; HRMS (ESI) (m/z) calcd for $\text{C}_{24}\text{H}_{26}\text{N}_3\text{O}_2$ [$\text{M} + \text{H}$]⁺ 388.2025, found 388.2024; IR (film) cm^{-1} 3853, 3748, 3673, 3650, 2959, 2922, 2852, 2360, 2340, 1734, 1699, 1652, 1612, 1557, 1540, 1509, 1363, 1197, 951, 859, 815, 715, 668.

Compound 10. (2.1 mg, 87%): TLC (EtOAc:*n*-hexane, 50:50 v/v) R_f = 0.48; ^1H NMR (400 MHz, CDCl_3) δ 8.11 (d, J = 8.4 Hz, 2H), 7.84 (d, J = 8.4 Hz, 2H), 7.58 (d, J = 9.0 Hz, 2H), 7.26 (s, 1H), 6.75 (d, J = 9.0 Hz, 2H), 6.44 (m, 1H), 3.59 (q, J = 6.6 Hz, 2H), 3.01 (s, 6H), 2.37 (t, J = 6.8 Hz, 2H), 1.86 (quint, J = 6.7 Hz, 2H), 0.13 (s, 9H); ^{13}C NMR (100 MHz, CDCl_3) δ 166.9, 158.9, 152.9, 150.6, 135.3, 130.4, 127.4, 126.0, 125.7, 121.0, 115.8, 112.2, 106.3, 85.9, 40.3, 39.6, 28.1, 17.8, 0.1; UV–vis λ_{max} 366 nm; Fluorescence λ_{max} (CH_2Cl_2) 508 nm; HRMS (ESI) (m/z) calcd for $\text{C}_{26}\text{H}_{32}\text{N}_3\text{O}_2\text{Si}$ [$\text{M} + \text{H}$]⁺ 446.2264, found 446.2262; IR (film) cm^{-1} 3853, 3748, 3673, 3650, 2921, 2360, 2340, 2175, 1734, 1699, 1652, 1613, 1558, 1540, 1508, 1363, 1106, 842, 761.

Synthesis of Compound 6. To a solution of Boc-protected **17**¹⁴ (9.0 mg, 35 μmol) in CH_2Cl_2 (1.0 mL) was added $\text{CF}_3\text{CO}_2\text{H}$ (0.2 mL), and the reaction mixture was stirred at 0 °C for 1 h. After concentration under reduced pressure, the residue was dissolved in CH_2Cl_2 (0.1 mL). To this solution was added a solution of **23** (3.0 mg, 7.4 μmol) in CH_2Cl_2 (0.1 mL), and the resulting mixture was stirred at 0 °C for 30 min. The mixture was diluted with EtOAc (3 mL), washed with saturated NH_4Cl (0.5 mL) and brine (0.5 mL), dried over MgSO_4 , filtered, and concentrated under reduced pressure. The crude product was purified by column chromatography to give **6** (2.9 mg, 86%): TLC (EtOAc:*n*-hexane, 50:50 v/v) R_f = 0.23; ^1H NMR (400 MHz, acetone- d_6) δ 8.15 (d, J = 8.6 Hz, 2H), 8.03 (d, J = 8.54 Hz, 2H), 7.95 (bs, 1H), 7.68 (d, J = 9.0 Hz, 2H), 7.45 (s, 1H), 6.98 (dt, J = 7.0, 15.6 Hz, 1H), 6.84 (d, J = 9.0 Hz, 2H), 5.90 (dt, J = 1.6, 15.6 Hz, 1H), 4.12 (q, J = 7.12 Hz, 2H), 3.47 (q, J = 6.8 Hz, 2H), 3.02 (s, 6H), 2.35 (ddd, J = 1.50, 7.2, 14.6 Hz, 2H), 1.82 (quint, J = 7.2 Hz, 2H), 1.23 (t, J = 7.10 Hz, 3H); ^{13}C NMR (100 MHz, acetone- d_6) δ 166.6, 159.6, 153.8, 151.8, 149.3, 136.9, 130.8, 128.65, 128.64, 126.3, 122.5, 121.9, 116.5, 114.7, 113.1, 60.3, 40.2, 39.8, 39.6, 28.7, 14.4; UV–vis

λ_{\max} 366 nm; Fluorescence λ_{\max} (CH₂Cl₂) 508 nm; HRMS (ESI) (*m/z*) calcd for C₂₆H₂₉NaN₃O₄ [M + Na]⁺ 470.2050, found 470.2046; IR (film) cm⁻¹ 3898, 3732, 3647, 2922, 2362, 2335, 1741, 1678, 1652, 1560, 1517, 1460, 1398, 1259, 1024, 796, 713, 673.

Synthesis of Compound 8. To a solution of iodide **24**¹⁵ (300 mg, 1.26 mmol) in DMF (1.0 mL) were added phthalimide (204 mg, 1.39 mmol) and K₂CO₃ (261 mg, 1.89 mmol), and the resulting mixture was stirred overnight at 50 °C. After cooling to room temperature the mixture was diluted with Et₂O (30 mL), washed with brine (5 mL × 2), dried over MgSO₄, filtered, and concentrated under reduced pressure. The crude product was purified by column chromatography to give ivory oil (260 mg). To a stirred solution of the obtained oil (260 mg) in THF (1.0 mL) was added H₂NNH₂·H₂O (80% in H₂O, 0.3 mL), and the mixture was allowed to stir overnight at 60 °C. After cooling to room temperature, the resulting mixture was diluted with Et₂O (25 mL), washed with 1 N NaOH (5 mL) and brine (5 mL), dried over MgSO₄, filtered, and concentrated. The crude product was purified by column chromatography to give yellow oil (81 mg). To a stirred solution of **23** (2.5 mg, 6.17 μmol) in CH₂Cl₂ (0.1 mL) was added a solution of the obtained yellow oil (10 mg) in CH₂Cl₂ (0.1 mL), and the resulting mixture was stirred at 0 °C for 30 min. The mixture was diluted with EtOAc (3 mL), washed with saturated NH₄Cl (0.5 mL) and brine (0.5 mL), dried over MgSO₄, filtered, and concentrated under reduced pressure. The crude product was purified by column chromatography to give **8** (2.1 mg, 90%): TLC (EtOAc:*n*-hexane, 50:50 v/v) *R_f* = 0.36; ¹H NMR (600 MHz, acetone-*d*₆) δ 8.15 (d, *J* = 8.4 Hz, 2H), 8.03 (d, *J* = 8.4 Hz, 2H), 7.94 (bs, 1H), 7.68 (d, *J* = 9.0 Hz, 2H), 7.45 (s, 1H), 6.84 (d, *J* = 9.0 Hz, 2H), 4.02 (q, *J* = 7.2 Hz, 2H), 3.50 (q, *J* = 6.6 Hz, 2H), 3.02 (s, 6H), 2.22 (t, *J* = 7.2 Hz, 2H), 2.07 (m, 2H), 1.77 (quint, *J* = 7.2 Hz, 2H), 1.30 (t, *J* = 7.2 Hz, 3H); ¹³C NMR (100 MHz, CDCl₃) δ 166.7, 158.9, 152.8, 150.6, 135.4, 130.3, 127.4, 126.0, 125.6, 121.0, 115.8, 112.2, 90.2, 74.1, 40.3, 39.8, 28.9, 15.3, 14.4, 1.03; UV-vis λ_{\max} 366 nm; Fluorescence λ_{\max} (CH₂Cl₂) 508 nm; HRMS (ESI) (*m/z*) calcd for C₂₅H₂₇NaN₃O₃ [M + Na]⁺ 440.1945, found 440.1949; IR (film) cm⁻¹ 3855, 3748, 3673, 2919, 2850, 2360, 2340, 2271, 1699, 1652, 1612, 1558, 1540, 1509, 1363, 1223, 1197, 1016, 815, 715.

Synthesis of Compound 27. To a stirred solution of **29**²⁹ (284 mg, 1.19 mmol) in CH₃CN (10 mL) were added **30**³⁰ (267 mg, 1.26 mmol) and K₂CO₃ (329 mg, 2.38 mmol), and the resulting mixture was refluxed for 2 days. After cooling to room temperature, NH₄Cl (30 mL) was added, and the layers were separated. The aqueous layer was extracted with EtOAc (20 mL × 3). Combined organic layer was dried over MgSO₄, filtered, and concentrated under reduced pressure. The crude product was purified by column chromatography to give **27** (178 mg, 54%) as colorless oil: TLC (EtOAc:*n*-hexane, 17:83 v/v) *R_f* = 0.4; ¹H NMR (400 MHz, CDCl₃) δ 7.67 (d, *J* = 8.4 Hz, 2H), 7.26 (d, *J* = 7.9 Hz, 2H), 5.62 (ddt, *J* = 16.5, 10.0, 6.4 Hz, 1H), 5.17–5.11 (m, 2H), 3.80 (d, *J* = 6.5 Hz, 2H), 3.25–3.17 (m, 2H), 2.39 (s, 3H), 2.34 (ddt, *J* = 7.6, 6.6, 2.5 Hz, 2H), 1.70 (t, *J* = 2.6 Hz, 3H); ¹³C NMR (100 MHz, CDCl₃) δ 143.2, 136.9, 133.0, 129.6, 127.1, 118.9, 77.4, 75.6, 51.0, 46.5, 21.4, 19.4, 13.3; HRMS (ESI) (*m/z*) calcd for C₁₅H₁₉NO₂S [M + Na]⁺ 300.1029, found 300.1029; IR (film) cm⁻¹ 2920, 1600, 1441, 1336, 1156, 1090, 985, 919, 812, 740, 661.

Synthesis of Compound 28. To a stirred solution of amine **31**³¹ (388 mg, 2.44 mmol) in CH₂Cl₂ (10 mL) were added *i*-Pr₂NEt (640 μL, 3.67 mmol) and acryloyl chloride (200 μL, 2.46 mmol) at 0 °C, and the mixture was warmed to room temperature. After 4 h, NH₄Cl (20 mL) was added, and the layers were separated. The aqueous layer was extracted with CH₂Cl₂ (15 mL × 3). Combined organic layer was dried over MgSO₄, filtered, and concentrated under reduced pressure. The crude product was purified by column chromatography to give compound **28** (480 mg, 93%) as colorless oil: TLC (EtOAc:Hexane, 20:80 v/v) *R_f* = 0.2; ¹H NMR (400 MHz, toluene-*d*₈) δ 7.09–6.97 (m, 5H), 6.31–6.26 (m, 2H), 5.29 (dd, *J* = 7.4, 5.5 Hz, 1H), 4.40 (s, 2H), 3.28 (t, *J* = 6.5 Hz, 2H), 2.16 (bs, 2H), 1.73 (t, *J* = 2.6 Hz, 1H); ¹³C NMR (100 MHz, toluene-*d*₈) δ 166.3, 138.4, 137.7, 129.0, 128.8, 127.7, 127.4, 81.9, 70.5, 51.0, 46.3, 18.7; HRMS (ESI) (*m/z*) calcd for C₁₄H₁₅NO [M + Na]⁺ 236.1046, found 236.1050; IR (film) cm⁻¹

3377, 3291, 2975, 2929, 2893, 1641, 1604, 1447, 1426, 1365, 1202, 1080, 1045, 972, 876.

Measurement of Time-Dependent Fluorescence Quenching Signal. The time-dependent fluorescence quenching signal was measured by a Shimadzu RF-5301PC fluorometer with excitation at 350 nm and an excitation and emission slit width of 2 nm. Samples were prepared with anhydrous CH₂Cl₂ and measured under Ar. A solution of a substrate in CH₂Cl₂ (3.0 mL) in a 10 × 10 mm quartz cuvette was placed in the temperature-controlled holder of the fluorometer, and the fluorescence spectrum at time zero was acquired. A Ru catalyst solution (3.0 mM in CH₂Cl₂) was added to the substrate solution using a syringe, and the fluorescence spectra were obtained as a function of time. The area of the fluorescence curve, designated the fluorescence intensity, was calculated.

Determination of *exo/endo*/Triene Ratio in the Enyne RCM Reaction. Ru catalyst (5 mol %) was added to a CH₂Cl₂ solution (0.3 M) of an enyne substrate. The reaction mixture was stirred under ethylene atmosphere (100 psi) at 40 °C for 20 h. The mixture was filtered through a silica gel pad and washed with diethyl ether. The filtrate was concentrated in vacuo, and the residue was purified by flash column chromatography on silica gel to identify the *exo*, *endo*, and triene products. The ratios of these products were determined by integration of the olefinic protons in the 400 MHz ¹H NMR spectra of the crude mixtures.

Characterization Data for Compounds 38, 42–44. **Compound 38.** Data: *R_f* (20% EtOAc/*n*-hexane) = 0.5; ¹H NMR (400 MHz, benzene-*d*₆) δ 7.68 (d, *J* = 8.2 Hz, 2H), 6.77 (d, *J* = 8.2 Hz, 2H), 6.19 (dd, *J* = 17.8, 11.2 Hz, 1H), 5.39 (d, *J* = 17.8 Hz, 1H), 5.00–4.84 (m, 3H), 4.71–4.70 (m, 2H), 3.94 (s, 2H), 3.64 (s, 2H), 1.88 (s, 3H), 1.57 (s, 3H); ¹³C NMR (100 MHz, benzene-*d*₆) δ 142.6, 140.9, 140.8, 138.1, 136.9, 129.5, 128.1, 127.9, 118.3, 115.0, 114.2, 54.0, 49.3, 21.0, 20.1; HRMS (ESI) (*m/z*) calcd for C₁₆H₂₁NO₂S [M + Na]⁺ 314.1185, found 314.1187; IR (film) cm⁻¹ 2922, 1598, 1341, 1159, 1100, 910, 812, 781, 661.

Compound 42. Data: *R_f* (33% EtOAc/*n*-hexane) = 0.32; ¹H NMR (400 MHz, CDCl₃) δ 7.33–7.25 (m, 5H), 6.47 (dd, *J* = 17.5, 10.7 Hz, 1H), 5.92 (s, 1H), 5.46 (d, *J* = 17.4 Hz, 1H), 5.37 (d, *J* = 10.6 Hz, 1H), 4.63 (s, 2H), 3.34 (t, *J* = 7.1 Hz, 2H), 2.44 (td, *J* = 7.1, 1.3 Hz, 2H); ¹³C NMR (100 MHz, CDCl₃) δ 166.0, 148.0, 138.0, 136.9, 129.2, 128.6, 128.0, 123.6, 119.5, 77.8, 50.2, 45.0, 23.8; HRMS (ESI) (*m/z*) calcd for C₁₄H₁₃NO [M + Na]⁺ 236.1046, found 236.1051; IR (film) cm⁻¹ 2925, 1654, 1622, 1586, 1479, 1445, 1423, 1343, 1326, 1247, 1173, 1074, 1029, 989, 924, 875, 798, 730, 699.

Compound 43. Data: *R_f* (33% EtOAc/*n*-hexane) = 0.34; ¹H NMR (400 MHz, CDCl₃) δ 7.32–7.25 (m, 5H), 6.46 (d, *J* = 12.7 Hz, 1H), 5.95 (d, *J* = 12.6 Hz, 1H), 5.19 (s, 1H), 5.06 (p, *J* = 1.6 Hz, 1H), 4.67 (s, 2H), 3.40–3.32 (m, 2H), 2.54–2.48 (m, 2H); ¹³C NMR (100 MHz, CDCl₃) δ 167.8, 144.7, 138.6, 137.9, 129.2, 128.8, 128.1, 124.9, 122.3, 77.8, 52.3, 46.8, 36.3, 30.3; HRMS (ESI) (*m/z*) calcd for C₁₄H₁₅NO [M + Na]⁺ 236.1046, found 236.1042; IR (film) cm⁻¹ 2922, 1635, 1612, 1578, 1481, 1435, 1356, 1261, 1227, 1196, 1159, 1094, 1026, 947, 913, 834, 802, 743, 700.

Compound 44. Data: *R_f* (33% EtOAc/*n*-hexane) = 0.5; ¹H NMR (400 MHz, toluene-*d*₈) δ 7.05–6.97 (m, 5H), 6.35–6.30 (m, 2H), 6.16 (dd, *J* = 17.6, 10.8 Hz, 1H), 5.30 (dd, *J* = 8.2, 4.7 Hz, 1H), 5.15 (d, *J* = 17.6 Hz, 1H), 4.90–4.84 (m, 2H), 4.77 (s, 1H), 4.37 (s, 2H), 3.32 (t, *J* = 7.8 Hz, 2H), 2.31 (t, *J* = 7.8 Hz, 2H); ¹³C NMR (100 MHz, toluene-*d*₈) δ 166.1, 144.6, 138.9, 138.7, 129.0, 127.6, 126.9, 116.8, 113.8, 51.0, 47.1, 31.5; HRMS (ESI) (*m/z*) calcd for C₁₆H₁₉NO [M + Na]⁺ 264.1359, found 264.1358; IR (film) cm⁻¹ 2931, 1644, 1605, 1433, 1365, 1220, 1159, 978, 902, 797, 736, 698.

■ ASSOCIATED CONTENT

Supporting Information

Time-dependent change of the fluorescence spectra, time-dependent quenching traces at various conditions, global fitting analysis of FRET data, and ¹H and ¹³C NMR spectra of new compounds. This material is available free of charge via the Internet at <http://pubs.acs.org>.

■ AUTHOR INFORMATION

Corresponding Author

*E-mail: sohnjh@cnu.ac.kr; leehy@kaist.ac.kr; hyotcherl.ihce@kaist.ac.kr.

Notes

The authors declare no competing financial interest.

■ ACKNOWLEDGMENTS

This work was supported by the NRF grant (No. 20110013842 and No. 20110029194) funded by Korean Ministry of Education, Science and Technology (MEST) and the Research Center Program (CA1201) of Institute for Basic Science (IBS) in Korea.

■ REFERENCES

- (1) For selected reviews on FRET, see: (a) Yuan, L.; Lin, W.; Zheng, K.; Zhu, S. *Acc. Chem. Res.* **2013**, *46*, 1462. (b) Gell, D. A.; Grant, R. P.; MacKay, J. P. *Adv. Exp. Med. Biol.* **2012**, *747*, 19. (c) Miyawaki, A. *Annu. Rev. Biochem.* **2011**, *80*, 357. (d) Wu, J.; Liu, W.; Ge, J.; Zhang, H.; Wang, P. *Chem. Soc. Rev.* **2011**, *40*, 3483. (e) Sapsford, K. E.; Berti, L.; Medintz, I. L. *Angew. Chem., Int. Ed.* **2006**, *45*, 4562. (f) Haugland, R. P. *The Handbook. A Guide to Fluorescent Probes and Labeling Technologies*, 10th ed.; Invitrogen: San Diego, CA, 2005.
- (2) For selected reviews on enyne RCM, see: (a) Li, J.; Lee, D. *Eur. J. Org. Chem.* **2011**, 4269. (b) Fischmeister, C.; Bruneau, C. *Beilstein J. Org. Chem.* **2011**, *7*, 156. (c) Mori, M. *Materials* **2010**, *3*, 2087. (d) Kotha, S.; Meshram, M.; Tiwari, A. *Chem. Soc. Rev.* **2009**, *38*, 2065. (e) Mori, M. *Adv. Synth. Catal.* **2007**, *349*, 121. (f) Diver, S. T. *Coord. Chem. Rev.* **2007**, *251*, 671. (g) Villar, H.; Frings, M.; Bolm, C. *Chem. Soc. Rev.* **2007**, *36*, 55. (h) Diver, S. T.; Giessert, A. J. *Chem. Rev.* **2004**, *104*, 1317.
- (3) (a) Sohn, J.-H.; Kim, K. H.; Lee, H.-Y.; No, Z. S.; Ihee, H. *J. Am. Chem. Soc.* **2008**, *130*, 16506. (b) Kim, K. H.; Ok, T.; Lee, K.; Lee, H.-S.; Chang, K. T.; Ihee, H.; Sohn, J.-H. *J. Am. Chem. Soc.* **2010**, *132*, 12027.
- (4) (a) Kitamura, T.; Sato, Y.; Mori, M. *Adv. Synth. Catal.* **2002**, *344*, 678. (b) Hansen, E. C.; Lee, D. *Acc. Chem. Res.* **2006**, *39*, 509. (c) Poulsen, C. S.; Madsen, R. *Synthesis* **2003**, 1.
- (5) (a) Hoye, T. R.; Donaldson, S. M.; Vos, T. J. *Org. Lett.* **1999**, *1*, 277. (b) Schramm, M. P.; Reddy, D. S.; Kozmin, S. A. *Angew. Chem., Int. Ed.* **2001**, *40*, 4274. (c) Lloyd-Jones, G. C.; Margue, R. G.; de Vries, J. G. *Angew. Chem., Int. Ed.* **2005**, *44*, 7442. (d) Diver, S. T.; Galan, B. R.; Giessert, A. J.; Keister, J. B. *J. Am. Chem. Soc.* **2005**, *127*, 5762. (e) Kim, S. H.; Bowden, N.; Grubbs, R. H. *J. Am. Chem. Soc.* **1994**, *116*, 10801. (f) Hansen, E. C.; Lee, D. *J. Am. Chem. Soc.* **2003**, *125*, 9582.
- (6) (a) Kinoshita, A.; Mori, M. *Synlett* **1994**, 1020. (b) Stragies, R.; Schuster, M.; Blechert, S. *Angew. Chem., Int. Ed.* **1997**, *36*, 2518. (c) Kitamura, T.; Sato, Y.; Mori, M. *Chem. Commun.* **2001**, 1258. (d) Lee, H.-Y.; Kim, B. G.; Snapper, M. L. *Org. Lett.* **2003**, *5*, 1855. (e) Núñez, A.; Cuadro, A. M.; Alvarez-Builla, J.; Vaquero, J. J. *Chem. Commun.* **2006**, 2690. (f) Dieltiens, N.; Moonen, K.; Stevens, C. V. *Chem.—Eur. J.* **2007**, *13*, 203.
- (7) The previous theoretical studies on enyne RCM using simplified models for the Ru complexes proposed that the alkene-initiated pathway is more favorable because the step of *ix* or *xii* formation displayed higher intrinsic barrier than that of *iii* formation in their calculation.^{7a} However, more recent computation suggested different conclusions that the higher bulk included in the Ru model, the lower the preference for the alkene-initiated pathway is.^{7b} (a) Lippstreu, J. J.; Straub, B. F. *J. Am. Chem. Soc.* **2005**, *127*, 7444. (b) Núñez-Zarur, F.; Solans-Monfort, X.; Rodríguez-Santiago, L.; Pleixats, R.; Sodupe, M. *Chem.—Eur. J.* **2011**, *17*, 7506.
- (8) (a) Lee, Y.-J.; Schrock, R. R.; Hoveyda, A. H. *J. Am. Chem. Soc.* **2009**, *131*, 10652. (b) Zhao, Y.; Hoveyda, A. H.; Schrock, R. R. *Org. Lett.* **2011**, *13*, 784.
- (9) Poater, A.; Solans-Monfort, X.; Clot, E.; Coperet, C.; Eisenstein, O. *J. Am. Chem. Soc.* **2007**, *129*, 8207.
- (10) Other FRET-based method for the detection of Pd complex formation was reported. Lim, S.-G.; Blum, S. A. *Organometallics* **2009**, *28*, 4643.
- (11) Mori, M.; Sakakibara, N.; Kinoshita, A. *J. Org. Chem.* **1998**, *63*, 6082.
- (12) Hoveyda, A. H.; Zhugralin, A. R. *Nature* **2007**, *450*, 243.
- (13) Lee, J.; Lee, H.; Sohn, J.-H. *Bull. Korean Chem. Soc.* **2011**, *32*, 3213.
- (14) Perron, J.; Joseph, B.; Mérour, J.-Y. *Tetrahedron Lett.* **2003**, *44*, 6553.
- (15) Funk, R. L.; Bolton, G. L.; Brummond, K. M.; Ellestad, K. E.; Stallman, J. B. *J. Am. Chem. Soc.* **1993**, *115*, 7023.
- (16) García-Fandiño, R.; Castedo, L.; Granja, J. R.; Cárdenas, D. J. *Dalton Trans.* **2007**, 2925.
- (17) Na, Y.; Song, J.-A.; Han, S.-Y. *Bull. Korean Chem. Soc.* **2011**, *32*, 3164.
- (18) Dye-conjugated substrates **1**, **2**, **6**, **7**, and **9**, whose functionalites are the components of enynes in Table 2, were tested; see Supporting Information.
- (19) Trost, B. M.; Breder, A.; O'Keefe, B. M.; Rao, M.; Franz, A. W. *J. Am. Chem. Soc.* **2011**, *133*, 4766.
- (20) Núñez-Zarur, F.; Solans-Monfort, X.; Rodríguez-Santiago, L.; Sodupe, M. *ACS Catal.* **2013**, *3*, 206.
- (21) Ferrer, C.; Raducan, M.; Nevado, C.; Claverie, C. K.; Echavarren, A. M. *Tetrahedron* **2007**, *63*, 6306.
- (22) Sashuk, V.; Grela, K. *J. Mol. Catal. A: Chem.* **2006**, *257*, 59.
- (23) Li, Q.; Yu, Z. -X. *Organometallics* **2012**, *31*, 5185.
- (24) Molander, G. A.; Dowdy, E. D. *J. Org. Chem.* **1998**, *63*, 8983.
- (25) Scheideman, M.; Wang, G.; Vedejs, E. *J. Am. Chem. Soc.* **2008**, *130*, 8669.
- (26) Tietze, L. F.; Bratz, M. *Chem. Ber.* **1989**, *122*, 977.
- (27) Li, Y.; Marks, T. J. *J. Am. Chem. Soc.* **1996**, *118*, 9295.
- (28) Diaz, L.; Bujons, J.; Casas, J.; Llebaria, A.; Delgado, A. *J. Med. Chem.* **2010**, *53*, 5248.
- (29) Fang, F.; Vogel, M.; Hines, J. V.; Bergmeier, S. C. *Org. Biomol. Chem.* **2012**, *10*, 3080.
- (30) Teichert, J. F.; Zhang, S.; van Zijl, A. W.; Slaa, J. W.; Minnaard, A. J.; Feringa, B. L. *Org. Lett.* **2010**, *12*, 4658.
- (31) Hess, W.; Burton, J. W. *Chem.—Eur. J.* **2010**, *16*, 12303.